RAPID COMMUNICATIONS

PHYSICAL REVIEW A VOLUME 52, NUMBER 6 DECEMBER 1995

Carbon geometry of $C_3H_3^+$ and $C_3H_4^+$ molecular ions probed by laser-induced Coulomb explosion

C. Cornaggia

Commissariat à l'Energie Atomique, Division des Sciences de la Matière, Service des Photons, Atomes et Molécules, F-91 191 Gif-Sur-Yvette, France

(Received 19 June 1995)

The structure of $C_3H_3^+$ and $C_3H_4^+$ ions produced by nonresonant multiphoton ionization is determined using laser-induced Coulomb explosion and associated multicharged atomic ion momenta correlations. Both cations exhibit the same C_3 average elongated linear carbon geometry. Stretched and bent nuclear configurations around the average structure are included in the calculations in order to reproduce the observed ion-ion correlation peak shapes.

PACS number(s): 33.80.Rv, 33.80.Eh, 42.50.Vk

The laser-induced Coulomb explosion of molecules has become possible with the advent of picosecond and femtosecond lasers, which can deliver intensities in the 10^{15}–10^{16} W/cm^2 laser intensity range, where the laser electric field is comparable to the molecular field experienced by valence electrons. The ejection of these outer electrons produces the explosion of the transient molecular ion into multicharged atomic ions:

$$[ABC^{M+}] \rightarrow A^{Z''+} + B^{Z'+} + C^{Z+} + (\text{ kinetic-energy release}).$$

Much experimental data has been published in the literature for diatomic molecules since the pioneering work of Frasinski *et al.* [1,2]. In particular, the whole fragmentation pattern is found to be independent of laser excitation conditions, such as the laser wavelength, pulse duration, and intensity [3]. For polyatomic ion species, such as CO_2^+ or $C_2H_2^+$, the multifragmentation into multicharged atomic ions is observed to be a direct process, with no intermediate daughter molecular ion formation [4,5]. The aim of this work is to determine the geometry of the carbon chain of the ion species $C_3H_4^+$ and $C_3H_3^+$ produced by nonresonant multiphoton ionization of allene, using laser-induced Coulomb explosion. In order to emphasize the C_3 carbon skeleton behavior for linear and bent structures, respectively, a comparison of the allene and propane multifragmentation patterns is presented. These experiments provide a direct determination of the molecular geometry in the intense laser field.

Molecular Coulomb explosion is produced by a 130-fs Ti:sapphire laser system operating at $\lambda = 790$ nm and focused intensities up to 2×10^{16} W/cm^2 (CEA/DRECAM laser facility). The single ionization occurs at the beginning of the laser pulse and then multiple ionization appears for higher instantaneous laser intensities. The resulting multicharged atomic and molecular ion species are detected by a Wiley-MacLaren short time-of-flight ion mass spectrometer [6], which is operated so that the ion time of flight T is a linear function of the projection of the ion initial momentum P along the spectrometer axis [5]. The $C^{Z''+} + C^{Z'+} + C^{Z+}$ fragmentation channels are identified using momenta statistical correlation techniques based on covariance mapping introduced by Frasinski *et al.* [2].

Figure 1 represents the mass spectra recorded with C_3H_4 and C_3H_8 molecules. For C_3H_4, the dominant molecular ion peaks are due to $C_3H_4^+$ and $C_3H_3^+$ cations and $C_3H_4^{2+}$ and $C_3H_2^{2+}$ dications. The contribution of the $C_2H_n^+$ ions is very weak in comparison with the detected $C_2H_p^+$ ions with $p = 2,3,4,5$ in the mass spectrum of C_3H_8. In the case of allene, four π electrons can absorb photons, while the C_3 carbon skeleton remains bound by σ electrons; hence the detection of $C_3H_4^{2+}$ and $C_3H_2^{2+}$ dications with two missing π electrons. In addition, the very weak $C_2H_n^+$ cation's con-

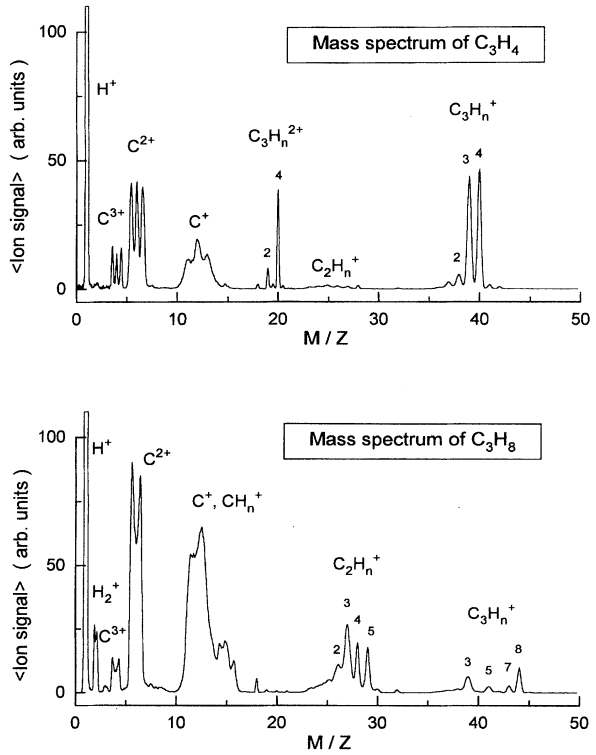

FIG. 1. Mass spectrum of C_3H_4 and C_3H_8 recorded at $\lambda = 790$ nm, $I = 2.5 \times 10^{15}$ W/cm^2, and $p = 10^{-9}$ Torr. The ratio M/Z represents the mass divided by the charge.

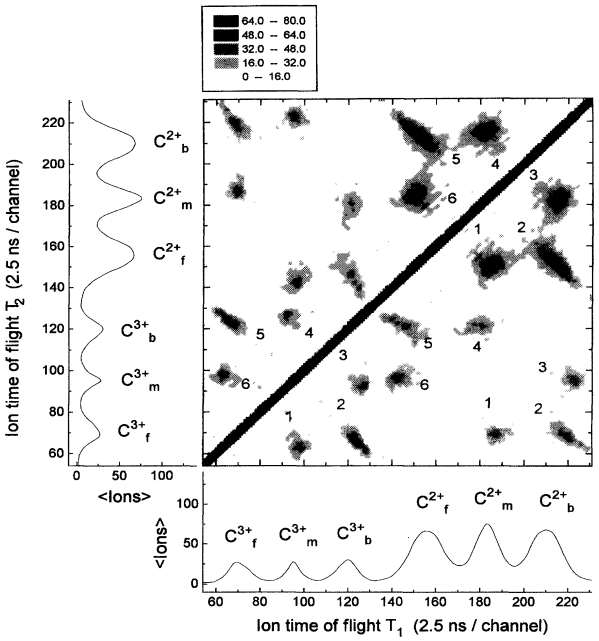

FIG. 2. Time-of-flight double-correlation map and associated time-of-flight spectra recorded for C_3H_4 at $\lambda = 790$ nm and $I = 5 \times 10^{15}$ W/cm^2. The double-correlation coefficient $R^{(2)}(T_1, T_2)$ is multiplied by 1000 and represented using a five-level gray scale as a function of the horizontal T_1 and vertical T_2 time-of-flight axes. Each $C^{Z'+}$-C^{Z+} ($Z', Z = 2,3$) correlation pattern exhibits a six-island pattern associated with the $C_f^{Z''+} + C_m^{Z'+} + C_b^{Z+}$ channel, where the subscripts f, m, and b correspond, respectively, to forward, middle, and backward ions registered by the spectrometer detector. No. 1: $C_f^{Z'+}$-C_m^{Z+} ; No. 2: $C_f^{Z'+}$-C_b^{Z+} ; No. 3: $C_m^{Z'+}$-C_b^{Z+} ; No. 4: $C_b^{Z'+}$-C_m^{Z+} ; No. 5: $C_b^{Z'+}$-C_f^{Z+} ; No. 6: $C_m^{Z'+}$-C_f^{Z+} .

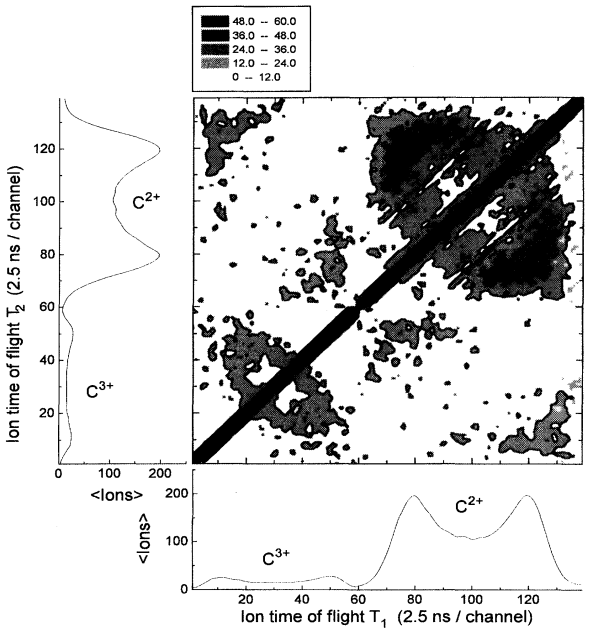

FIG. 3. Time-of-flight double-correlation map and associated time-of-flight spectra recorded for C_3H_8 at $\lambda = 790$ nm and $I = 5 \times 10^{15}$ W/cm^2.

tribution to the mass spectrum is a clear signature of the direct instantaneous multifragmentation of the C_3 chain with no intermediate production of daughter molecular ions. For propane, only σ electrons are coupled to the laser field. When they are excited to σ^* orbitals or to the continuum, the molecule becomes highly unstable, so that we detect $C_2H_p^+$ and CH_q^+ coming from the rupture of the C_3 carbon chain.

In Figs. 2 and 3, the conventional C^{2+} and C^{3+} time-of-flight spectrum is placed along the ion time-of-flight axes T_1 and T_2. For allene (Fig. 2), the carbon C^{Z+} ions exhibit a triple-ion peak structure that is due to ions with initial momentum headed toward the detector (forward ions C_f^{Z+}), away from the detector (backward ions C_b^{Z+}), and ions with little initial momentum, which come from the middle carbon atom (C_m^{Z+}). The islands in the central map represent ion-ion correlation peaks, which involve ions of time of flight T_1 for the horizontal axis and T_2 for the vertical one. For each $C^{Z'+}$-C^{Z+} correlation location, a six-island pattern is detected and corresponds to the different pair of ions belonging to the $C_f^{Z''+} + C_m^{Z'+} + C_b^{Z+}$ fragmentation channel. Triple $C^{Z''+}$-$C^{Z'+}$-C^{Z+} correlations were recorded at a lower time-of-flight resolution for a complete assignment of the explosion channels of the C_3 chain of C_3H_4. Table I summarizes the detected channels and the corresponding kinetic-energy releases, which are measured at the maxima of the correlation coefficients. For a particular channel $C^{Z''+} + C^{Z'+} + C^{Z+}$, the kinetic-energy release spectrum exhibits only one maximum. In consequence, the geometries of $C_3H_4^+$ and $C_3H_3^+$ precursor molecular ions are similar; otherwise several maxima would be observed. In Table I, the measured kinetic-energy releases that are lower than expected from a pure Coulomb repulsion and constant ratios $E_{\text{expt}}/E_{\text{Coul}}$ are common features of laser-induced Coulomb explosion of diatomic and polyatomic ion species. The simplest explanation is to consider that Coulomb explosion occurs at larger internuclear distances R_c than the equilibrium distances R_e^+ due to the $1/R$ dependence of the Coulomb repulsion potential. Here $R_c = 2.1\ R_e^+$, where the 2.1 factor is the inverse of the 0.47 average value of the $E_{\text{expt}}/E_{\text{Coul}}$ ratios. Since these ratios remain nearly constant whatever the charge state of the exploding channel (Table I), the successive ionization steps of the initial molecular cation do not modify the geometry from one ionization event to the next one. These observations are in good agreement with two recent models based, respectively, on field-ionization [7] and on quantum time-dependent calculations [8]. Both approaches predict that Coulomb explosion is dramatically enhanced at critically larger internuclear distances than the equilibrium internuclear distances of the unperturbed molecular ion.

Since the measurements of the ejected ions' momenta give information on the positions of the atoms within the exploding molecule, the following simple model is compared with the experimental data. The geometry of the C_3 chain is given by the internuclear distance between the carbon atoms $R = R(\text{C-C})$ and the angle γ between the two C—C bonds. The momenta $P(R, \gamma)$ of the ions belonging to the $C^{Z''+} + C^{Z'+} + C^{Z+}$ channel are calculated as the results of a pure

TABLE I. Fragmentation channels of allene identified from double- and triple-correlation experiments. E_{expt} is the measured kinetic-energy release at the maximum of the correlation coefficient for each ion component of the $C^{Z''+}+C^{Z'+}+C^{Z+}$ channel. The relative accuracy is 5% except for the middle carbon ions $C_m^{Z'+}$ for which the kinetic energies remain very weak. E_{Coul} represents the corresponding calculated energy for Coulomb explosion of the C_3 linear chain starting at the R_e^+(C-C) equilibrium internuclear distance of the $C_3H_4^+$ ion. The ratios E_{expt}/E_{Coul} are expressed in percentages.

Channel	Ion	E_{expt} (eV)	E_{Coul} (eV)	E_{expt}/E_{Coul} (%)
	C^{2+}	25	54.1	46
$C^{2+}+C_m^{2+}+C^{2+}$	C_m^{2+}	0	0	
	C^{2+}	25	54.1	46
	C^{3+}	36	74.4	49
$C^{3+}+C_m^{2+}+C^{2+}$	C_m^{2+}	0.1	0.24	
	C^{2+}	32	66.1	48
	C^{2+}	36	75.7	48
$C^{2+}+C_m^{3+}+C^{2+}$	C_m^{3+}	0	0	
	C^{2+}	36	75.7	48
	C^{3+}	40	89.3	45
$C^{3+}+C_m^{2+}+C^{3+}$	C_m^{2+}	0	0	
	C^{3+}	40	89.2	45
	C^{3+}	48	102.6	47
$C^{3+}+C_m^{3+}+C^{2+}$	C_m^{3+}	0.4	0.3	
	C^{2+}	41	91.8	45
	C^{3+}	57	121.7	47
$C^{3+}+C_m^{3+}+C^{3+}$	C_m^{3+}	0	0	
	C^{3+}	57	121.7	47

Coulomb repulsion between these ions. The classical equations of motion are solved for each initial (R,γ) couple in the molecular frame. Bent geometries around the linear structure are introduced with γ angles different from 180°. The momenta can be represented by their moduli $P(R,\gamma)$ and angles $\beta(R,\gamma)$ with the molecular Z axis. For parallel detection axis and laser polarization direction, the detected momenta are given by $P_d=P(R,\gamma)\cos[\theta+\beta(R,\gamma)]$, where θ is the angle between the Z axis of the molecular frame and the detection axis. Bent configurations are assumed to take place in the plane defined by the laser polarization axis and the initial linear C_3 chain, where the molecular rotation takes place. Figure 4 represents the calculated double-correlation time-of-flight spectrum for allene. The average geometrical initial conditions are $R_c=2.1R_e^+$(C-C) and $\gamma_c=180°$, where R_e^+(C-C) is the carbon-carbon internuclear distance of the linear nonperturbed $C_3H_4^+$ ion, and the 2.1 factor stands for the observed elongated shape of the molecular structure. Bent and stretched configurations around these values are

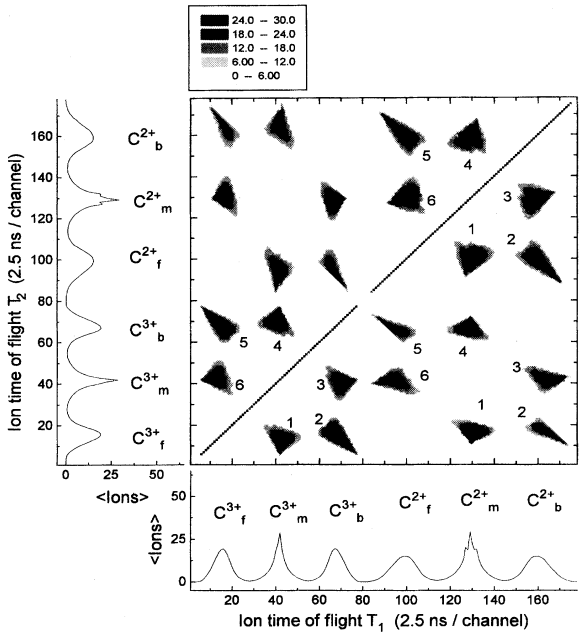

FIG. 4. Calculated time-of-flight double-correlation spectrum for a linear $C_3H_4^+$ ion. The spectrometer operating conditions and island labels are the same as in Fig. 2.

introduced using simple triangular distributions peaked at R_c and γ_c, with respective total extensions from $0.5R_c$ to $1.5R_c$ for R and from 140° to 220° for γ. The molecular alignment is represented by a triangular θ distribution peaked at $\theta_c=0°$, with a total extension from −40° to 40°. These values were chosen to fit the experimental data and no effort was made to normalize the results, since we are mainly interested in correlation locations. The agreement between the calculated and the observed correlations is good and confirms the linear exploding configuration of the detected $C_3H_4^+$ and $C_3H_3^+$ ions. The extensions of the correlation islands are due to different geometries around the average linear structure. Moreover, the linear configuration calculations do not reproduce the observed correlation map recorded with propane represented in Fig. 3. The observed elliptical shapes of the correlation islands come from the bent structure and possible sequential multifragmentation and remain to be investigated in more detail.

In conclusion, the carbon geometry of $C_3H_4^+$ and $C_3H_3^+$ ions produced by nonresonant multiphoton ionization is shown to be identically linear. The maxima of the kinetic-energy release spectra show that the molecular ions explode preferentially for elongated internuclear distances, in good agreement with two recent theoretical models [7,8]. Finally, this work is a first step forward using laser-induced Coulomb explosion as a tool for stereostructure studies of small polyatomic ions.

The author is pleased to acknowledge P. d'Oliveira and P. Meynadier for operating the CEA/DRECAM laser system and M. Bougeard and E. Caprin for their skilled technical assistance.

[1] L. J. Frasinski, K. Codling, P. Hatherly, J. Barr, I. N. Ross, and W. T. Toner, Phys. Rev. Lett. **58**, 2424 (1987).

[2] K. Codling and L. J. Frasinski, J. Phys. B **26**, 783 (1993), and references therein.

[3] C. Cornaggia, J. Lavancier, D. Normand, J. Morellec, P. Agostini, J. P. Chambaret, and A. Antonetti, Phys. Rev. A **44**, 4499 (1991).

[4] C. Cornaggia, M. Schmidt, and D. Normand, J. Phys. B **27**, L123 (1994).

[5] C. Cornaggia, M. Schmidt, and D. Normand, Phys. Rev. A **51**, 1431 (1995).

[6] W. C. Wiley and I. H. McLaren, Rev. Sci. Instrum. **26**, 1150 (1955).

[7] J. H. Posthumus, L. J. Frasinski, A. J. Giles, and K. Codling, J. Phys. B **28**, L349 (1995).

[8] T. Seideman, M. Yu. Ivanov, and P. B. Corkum, Phys. Rev. Lett. **75**, 2819 (1995).

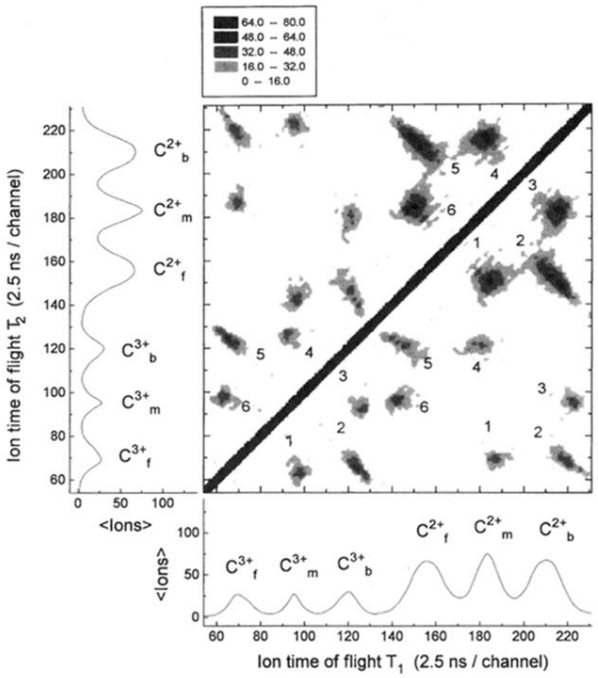

FIG. 2. Time-of-flight double-correlation map and associated time-of-flight spectra recorded for C_3H_4 at $\lambda = 790$ nm and $I = 5 \times 10^{15}$ W/cm^2. The double-correlation coefficient $R^{(2)}(T_1, T_2)$ is multiplied by 1000 and represented using a five-level gray scale as a function of the horizontal T_1 and vertical T_2 time-of-flight axes. Each $C^{Z'+}$-C^{Z+} $(Z', Z = 2,3)$ correlation pattern exhibits a six-island pattern associated with the $C_f^{Z'+} + C_m^{Z'+} + C_b^{Z+}$ channel, where the subscripts f, m, and b correspond, respectively, to forward, middle, and backward ions registered by the spectrometer detector. No. 1: $C_f^{Z'+}$-C_m^{Z+} ; No. 2: $C_f^{Z'+}$-C_b^{Z+} ; No. 3: $C_m^{Z'+}$-C_b^{Z+} ; No. 4: $C_b^{Z'+}$-C_m^{Z+} ; No. 5: $C_b^{Z'+}$-C_f^{Z+} ; No. 6: $C_m^{Z'+}$-C_f^{Z+} .

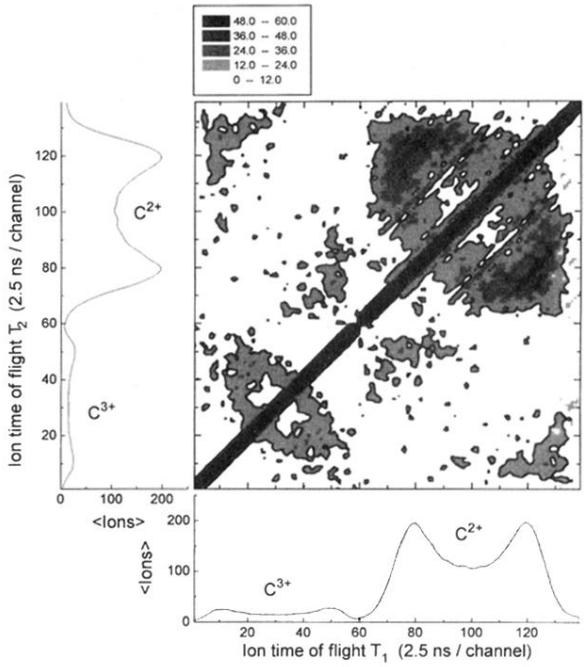

FIG. 3. Time-of-flight double-correlation map and associated time-of-flight spectra recorded for C_3H_8 at $\lambda = 790$ nm and $I = 5 \times 10^{15}$ W/cm^2.

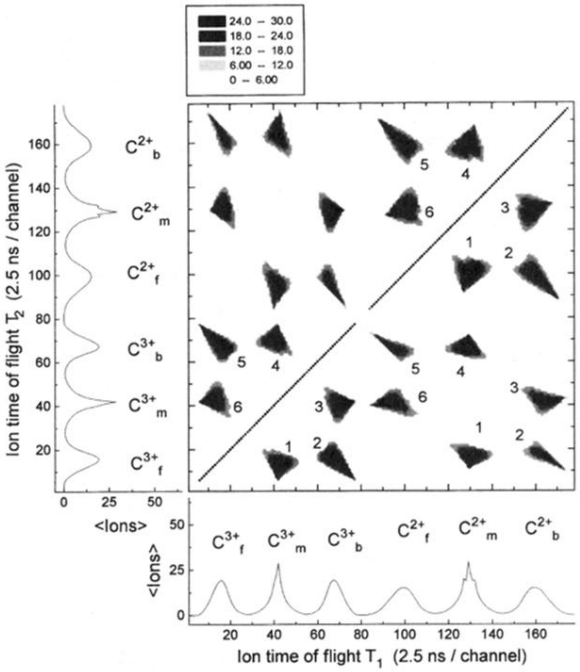

FIG. 4. Calculated time-of-flight double-correlation spectrum for a linear $C_3H_4^+$ ion. The spectrometer operating conditions and island labels are the same as in Fig. 2.